PROCEEDINGS OF SPIE

SPIEDigitalLibrary.org/conference-proceedings-of-spie

Metrology of thin resist for high NA EUVL

Gian Francesco Lorusso, Christophe Beral, Janusz Bogdanowicz, Danilo De Simone, Mahmudul Hasan, et al.

Gian Francesco Lorusso, Christophe Beral, Janusz Bogdanowicz, Danilo De Simone, Mahmudul Hasan, Christiane Jehoul, Alain Moussa, Mohamed Saib, Mohamed Zidan, Joren Severi, Vincent Truffert, Dieter Van den Heuvel, Alex Goldenshtein, Kevin Houchens, Gaetano Santoro, Daniel Fischer, Angelika Muellender, Joey Hung, Roy Koret, Igor Turovets, Kit Ausschnitt, Chris Mack, Tsuyoshi Kondo, Tomoyasu Shohjoh, Masami Ikota, Anne-Laure Charley, Philippe Leray, "Metrology of thin resist for high NA EUVL," Proc. SPIE 12053, Metrology, Inspection, and Process Control XXXVI, 120530O (26 May 2022); doi: 10.1117/12.2614046

SPIE.

Event: SPIE Advanced Lithography + Patterning, 2022, San Jose, California, United States

Metrology of Thin Resist for High NA EUVL

Gian Francesco Lorusso[a], Christophe Beral[a], Janusz Bogdanowicz[a], Danilo De Simone[a], Mahmudul Hasan[a], Christiane Jehoul[a], Alain Moussa[a], Mohamed Saib[a], Mohamed Zidan[a], Joren Severi[a], Vincent Truffert[a], Dieter Van Den Heuvel[a], Alex Goldenshtein[b], Kevin Houchens[b], Gaetano Santoro[b], Daniel Fischer[c], Angelika Muellender[c], Joey Hung[d], Roy Koret[d], Igor Turovets[d], Kit Ausschnitt[e], Chris Mack[f], Tsuyoshi Kondo[g], Tomoyasu Shohjoh[g], Masami Ikota[g], Anne-Laure Charley[a], Philippe Leray[a]

[a]imec, Kapeldreef 75, 3001 Leuven, Belgium;
[b]Applied Materials, 8, Prof. A. D. Bergman St 4, Rehovot, Israel;
[c]Carl Zeiss SMT GmbH, Carl-Zeiss-Straße 22, 73447 Oberkochen, Germany;
[d]NOVA, 5 David Fikes St., Rehovot 7632805, Israel;
[e]KAC, Round Pond, Maine, USA;
[f]Fractilia, Austin Texas, USA;
[g]Hitachi High-Tech Corp., Japan.

Abstract:

One of the many constrains of High Numerical Aperture Extreme Ultraviolet Lithography (High NA EUVL) is related to resist thickness. In fact, one of the consequences of moving from current 0.33NA to 0.55NA (high NA) is the Depth of Focus (DOF) reduction. In addition, as the resist feature lines shrink down to 8nm half pitch, it is essential to limit the aspect ratio to avoid pattern collapse. The direct consequence of such a situation is that a resist thickness of 30nm, usually used for 32nm pitch dense line/space (LS), will not be suitable for 16nm pitch, where the target thickness is expected to be 15nm thickness or less to ensure a similar aspect ratio.

The question we need to answer is how the resist thickness reduction will impact the various metrology techniques needed to properly set up a process. To address this question, a set of wafers using both Chemical Amplified Resist (CAR) and Metal Oxide Resist (MOR) at different thicknesses and with different types of underlayer have been generated for LS patterns at 32nm pitch. We first investigated the impact of film thickness by scanning electron microscope (SEM) on the imaging of CAR resist lines. To start with, our current Best-Known Methods (BKM's) were used to acquire the SEM images. As resist thickness decreases, noise level and image contrast are observed to degrade dramatically. Such an image quality degradation may directly impact the quality of the CD measurements both in terms of accuracy and precision.

In this paper we investigated the thin resist wafer set described above using various techniques, such as Critical Dimension Scanning Electron Microscope (CD SEM), Atomic Force Microscopy (AFM), Low Voltage SEM (LV SEM), scatterometry, Pattern Shift Response (PSR), and optical defect inspection. The impact of the resist thickness is estimated for each approach, and optimal settings were investigated to minimize the relative impact on metrology. Our results indicated that, in most cases, alternative operation conditions and BKM settings, sometimes drastically different from the usual operation condition, must be used to guarantee the metrology requirements. Our results show that, despite the impact of thinning resist materials, it is possible to find appropriate settings to strengthen the metrology quality output.

Keywords: Thin Resist, High NA EUVL, e-beam, CD SEM, Scatterometry, AFM, inspection, PSR

Metrology, Inspection, and Process Control XXXVI, edited by John C. Robinson, Matthew J. Sendelbach,
Proc. of SPIE Vol. 12053, 120530O · © 2022 SPIE · 0277-786X · doi: 10.1117/12.2614046

1. INTRODUCTION

Wavelength scaling has been one of the main techniques used to enhance lithographic performance in the semiconductor industry, ultimately ensuring the survival of Moore's law for many years. From the i-line (365nm) in the early 90's, the industry moved to KrF (248nm), ArF (193nm), and finally EUV (13.5nm), allowing to drop the minimum feature on wafer from 350nm down to 16nm. Wavelength scaling is a consequence of the first Rayleigh equation (1):

$$CD = k_1 \frac{\lambda}{NA} \quad (1)$$

being CD the critical dimension, k_1 a coefficient that depends on many factors related to the chip manufacturing process, and NA the numerical aperture. It is evident that, by reducing the wavelength λ, the printed CD will become smaller and smaller. But there is more than one way to get there. In the late 2000's, the scaling was achieved by transitioning from ArF to ArF immersion. In this case, the wavelength was kept constant, but the increase of NA in water as compared to air was used to drive performances, thus enabling NA scaling. What High NA EUVL is going to do is something similar.

There is also a second Rayleigh equation, dealing with the impact of wavelength and numerical aperture on depth of focus (2):

$$DOF = k_2 \frac{\lambda}{NA^2} \quad (2)$$

where DOF is the depth of focus and k_2 is another process-dependent constant. Looking at eq. (2), we observe a critical difference between wavelength and numerical aperture scaling. When the wavelength is reduced, the DOF decreases linearly with it. By contrast, when NA is increased, the DOF decreases as the square of it. This implies a greater reduction of focus latitude in the case of NA scaling.

One way to reduce the impact of high NA on DOF is to adopt thinner resist. The adoption of thin resist is also critical to keep the aspect ratio small, which is essential to avoid pattern collapse. Currently, a resist thickness of about 30nm is used to print features around 16nm, with an aspect ratio of about 2. In the case of high NA, where the feature size on wafer is expected to drop below 10nm, a resist thickness of 15nm or below is likely to be used.

Using thin resist is not trivial for many reasons, as we need to ensure pattern quality, etch resistance, and more. The question we will try to address in this work is how the resist thickness reduction will impact the various metrology techniques needed to properly set up the process. To address this question, a set of wafers using both Chemical Amplified Resist (CAR) and Metal Oxide Resist (MOR) at different thicknesses and with different types of underlayer have been generated for LS patterns at 32nm pitch. We investigated the thin resist wafer set with various metrology techniques, such as Critical Dimension Scanning Electron Microscope (CD SEM), Atomic Force Microscopy (AFM), Low Voltage SEM (LV SEM), scatterometry, Pattern Shift Response (PSR), and optical defect inspection. The impact of the resist thickness is estimated for each approach, and optimal settings were investigated to minimize the relative impact on metrology.

2. RESULTS AND DISCUSSION - E-BEAM

2.1 BKM e-beam Metrology

We will start investigating the impact of reducing Film Thickness (FT) by using imec BKM for After Development Inspection (ADI) wafers [1]. The images are acquired at 500eV, 8pA, 16 frames, using a Hitachi CG6300. No attempt to improve the quality of the electron images by altering the BKM settings is done for now, as the main goal is to understand the limitation of our current BKM when imaging thin resist and the physical mechanism impacting metrology.

In Fig. 1(a), images of Chemical Amplified Resist (CAR) on Spin-on-Glass (SOG) underlayer at different Target FT, ranging from 10 up to 30nm, are reported. The impact of reducing resist FT on the images is evident. First and foremost, we observe that the noise level in the images increases when the film thickness is reduced. The effect can be quantified measuring the grayscale image noise versus resist thickness [8]. Such an effect is indeed expected. In fact, by decreasing the film thickness, the intersection between the interaction volume of the impinging beam and the resist feature is reduced as well, so that the secondary electron signal becomes lower. In the case of the smallest Target FT of 10nm, the line space (LS) pattern is barely visible. In this case, however, it is not clear for now if such a poor image is caused by the fact that the patterning itself is poor, or that the BKM used is not suitable for such an extreme condition. To clarify this point, reference measurement using Atomic Force Microscopy (AFM) were performed and will be discussed in Sec. 2.2.

In Fig. 1(b) we investigate the same CAR as in Fig. 1(a), this time on an organic underlayer (UL1) instead of SOG. Also in this case, the impact of reducing the resist FT consists in a deterioration of the contrast in the images, as for CAR on SOG. However, it is also evident that CAR on UL1 has better Signal-to-Noise Ratio (SNR) as compared to CAR on SOG, indicating that the impact on thickness on e-beam imaging is stack and material dependent. As the actual FT for CAR on SOG and CAR on UL1 is indeed similar, as confirmed by AFM measurements, we can speculate that the effect is a consequence of different charging characteristics of SOG as compared to UL1.

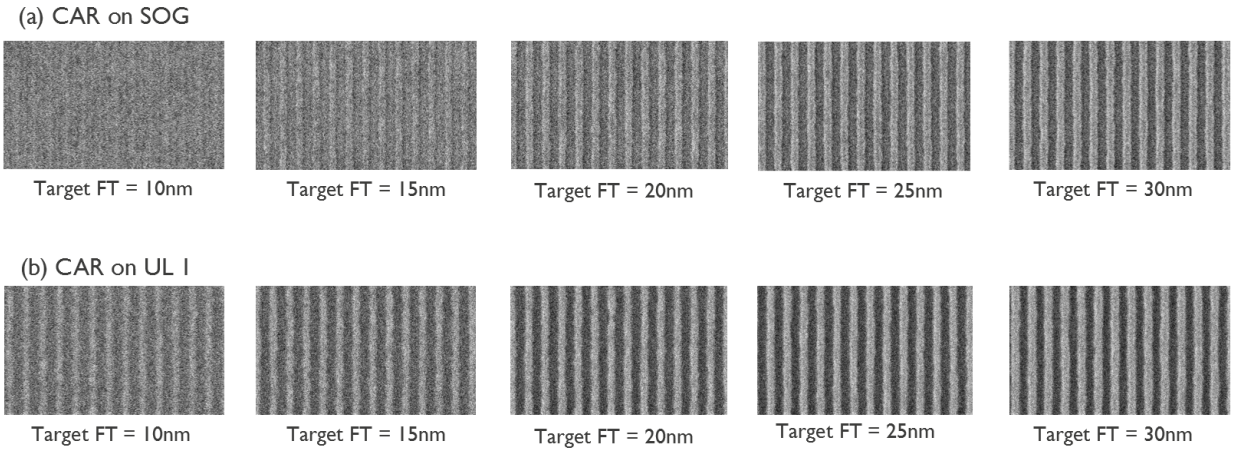

Figure 1. (a) Impact of reducing FT of CAR on SOG. (b) Impact of reducing resist FT of CAR on UL1. In both cases, the contrast is observed to decrease when the film thickness is decreased. Standard imec BKM's have been used and no attempt was made to improve imaging.

The results in Fig. 1 indicate that the choice of stack can greatly influence the imaging performance. This is confirmed in Fig. 2, where we compare SOG (a) to two different organic underlayer UL1 and UL2, (b) and (c) respectively. A target FT of 15nm is used in all cases shown in Fig. 2, and again no attempt to improve the quality of the electron images by altering the BKM settings is done, as this investigation is mainly intended to baseline and understand the impact on e-beam imaging for now. In Fig. 2 we observe that dramatic differences in image quality is not only present between SOG and organic underlayers [(a) and (b)], but it can also happen between two different types of organic underlayers [(b) and (c)], suggesting a complex relationship between the material in the stack and the e-beam image quality, likely related to charging artifacts.

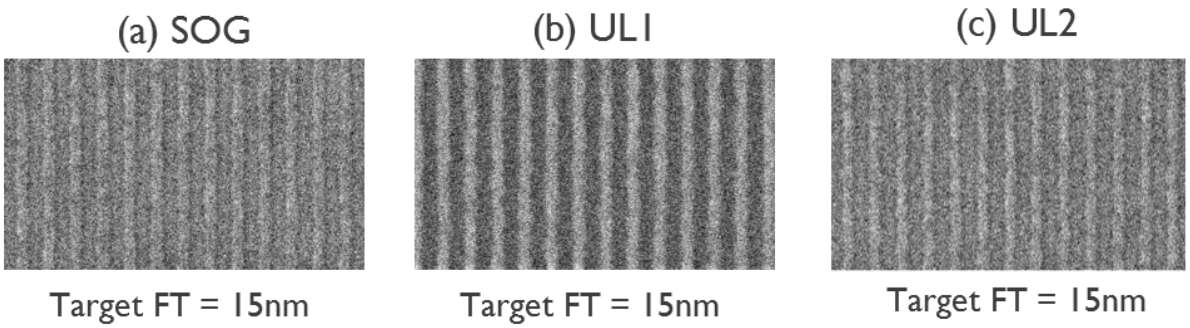

Figure 2. e-beam images of CAR patterns on different underlayers: SOG (a), UL1 (b) and UL2 (c). The patters were printed aiming for the same target resist FT (15nm). When comparing e-beam imaging at the same film thickness, UL1 shows higher contrast as compared to SOG and UL2. In all cases, standard imec BKM's have been used and no attempt was made to improve imaging.

In Fig. 3 we investigate the impact of target resist FT on Metal Oxide Resist (MOR) on SOG (a) and UL1 (b), respectively, as we have done in Fig. 1 for CAR. Again, no attempt to improve imaging by altering the BKM settings is done. Also in this case, we observe that the noise level increases when decreasing target FT. As for CAR, we observe better imaging performances for UL1 as compared to SOG. In the case of MOR, even the 10nm target FT on SOG is visible, while it was not for CAR. Basically, the results for MOR in Fig. 3 are consistent with the results for CAR in Fig. 1, but with one main difference, that MOR shows better Signal-to-Noise Ratio (SNR) as compared to CAR, within the constraints of the standard BKM used up to now.

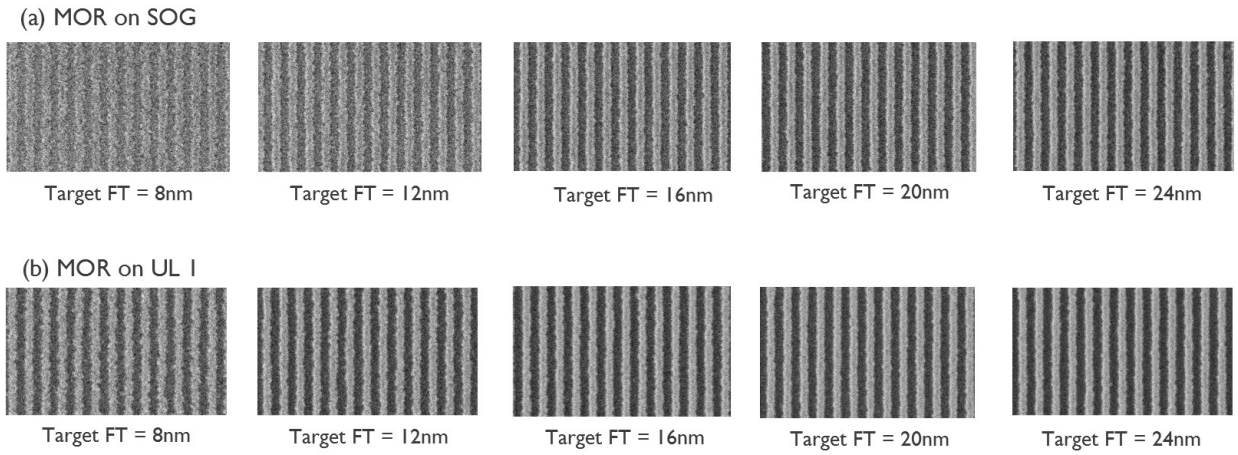

Figure 3. (a) Impact of reducing resist FT of MOR on SOG. (b) Impact of reducing FT of MOR on UL1. Impact of the nominal film thickness on e-beam images for MOR resist on SOG (a) and UL 1 (b). In both cases, the contrast is observed to decrease when film thickness is decreased. Imec standard BKM's were used for the Hitachi CG6300 imaging. Standard imec BKM have been used and no attempt was made to improve imaging.

2.2 AFM analysis

As discussed in Chap. 2.1, the poor quality of the results for CAR on SOG for the thinner resist FT [Fig. 1(a), Target FT = 10nm] leaves the door open to two distinct interpretations. The first, that the poor image quality observed is caused by the metrology settings, which are not optimized for the specific thin resist use case. Alternatively, it could be possible that the poor quality of the image is simply reflective of the poor quality of the patterning, meaning that the fact that we do not see any line is possibly an indication that simply there are no lines printed on wafer.

In order to be able to decide between these two options, we investigated the CAR on SOG patterns reported in Fig. 1(a) using AFM. The results are reported in Fig. 4. The AFM images have 1μm field of view (FOV). The results in Fig. 4 clearly indicate the presence of LS patterns even at target FT of 10nm, thus clarifying that the issue observed in Fig. 1(a) is a metrology issue, rather than a patterning one.

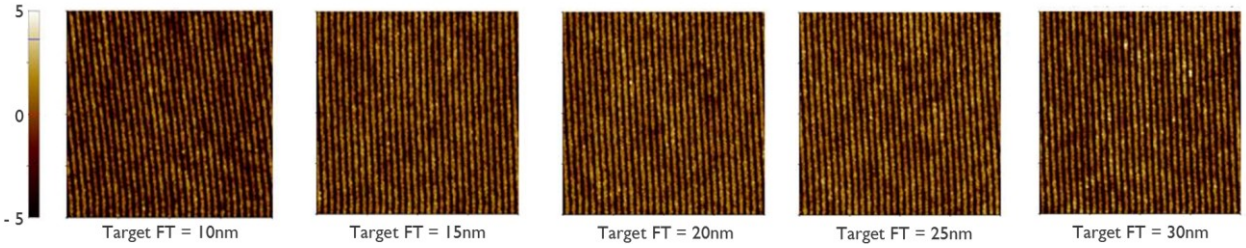

Figure 4. AFM images of CAR on SOG at different film thicknesses, corresponding to the e-beam images reported in Fig. 1(a). The AFM analysis shows that LS patterns are printed down to 10nm film thickness, thus indicating that the limitations observed in Fig. 1 (a) at 10nm target FT are related to metrology rather than patterning.

2.3 Impact of landing energy

The results discussed in Chap. 2.1 were all acquired using the standard imec protocol BKM [1], originally designed for features thicker than those investigated here. Having clarified in Chap. 2.2 that the poor imaging is a metrology issue rather than a patterning problem, our goal now is to understand how it is possible to extend the BKM to cover the use case of thin resist features. To this aim, we will investigate in the following the impact of Landing Energy (LE). LE is expected to impact various parameters related to e-beam imaging, such as interaction volume, charging, and shrinkage. Specifically, by modifying the interaction volume of the impinging electron, it is possible to alter the overlap between interaction volume and resist features, ultimately impacting the SNR of the e-beam images.

We used an aberration-corrected Low Voltage Scanning Electron Microscope (LV-SEM) from Zeiss [2] to investigate the impact of LE on thin resist [3]. Such a tool can perform at very low LE while retaining a resolution of 0.6nm. In Fig. 5 we report a set of images acquired with the Zeiss LV-SEM of CAR resist on SOG as a function of LE. Target FT is 15nm, images acquired at 24 frames. In the case of CAR, contrast is observed to improve by lowering the landing energy, because of the better overlap between interaction volume and LS features.

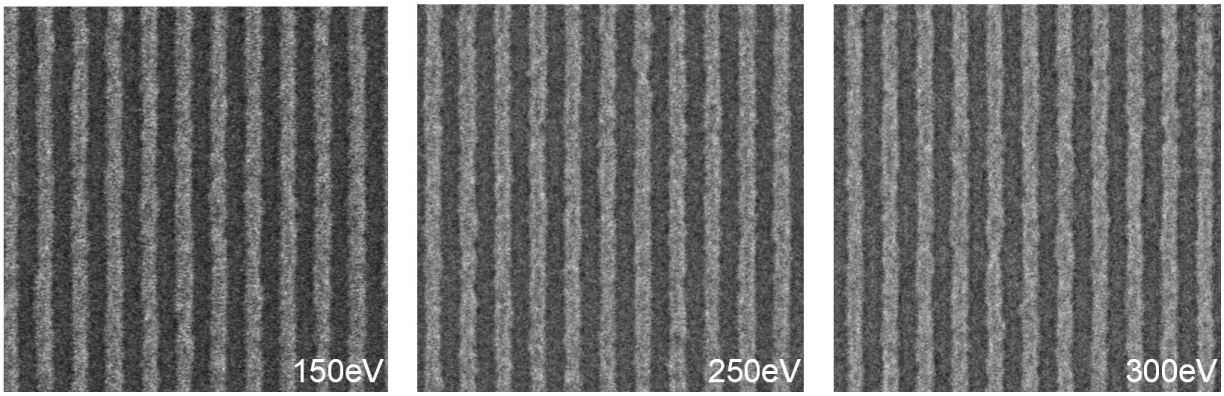

Figure 5. Zeiss Low-Voltage Aberration-Corrected SEM images of CAR on SOG, at a target FT of 15nm. The contrast is observed to improve by lowering the landing energy.

However, the interaction volume is not the only parameter to change when varying LE. To better understand the impact of LE on the physical condition at wafer level, in Fig. 6 we report how CD changes through dose at different LE.

The dose is modified by altering the number of frames, from 6 up to 24. From Fig. 6 we evince the existence of two distinct regimes in the energy range of interest investigated here. We see a high energy regime (a) dominated by shrinkage. In this regime, as we increase the dose by augmenting the number of frames, the CD is observed to become smaller. This well-known effect of resist shrinkage is de facto caused by physical damages induced in the resist by the electron beam at these relatively high LE. On the opposite side of the spectrum, we have a low energy regime (b) dominated by charging. In this regime, as we increase the dose by augmenting the number of frames, the CD is observed to become larger. This is a known artifact caused by the interaction of a low energy electron beam with a positively charged surface. We can identify, in between the two extremes, an equilibrium point (c) where the two effects of charging and shrinkage compensate each other, indicated approximately by the dashed line in Fig. 6.

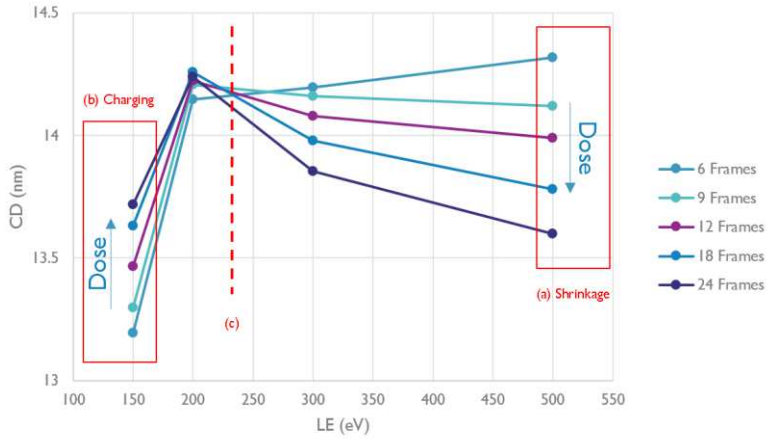

Figure 6. Impact of landing energy on CD for 15nm target FT of CAR on SOG. We clearly distinguish three different regimes. (a) A shrinkage regime is observed at high LE, where the CD decreases as the dose is increased. (b) A charging regime appears at low LE (where CD increases as the dose is increased). (c) the equilibrium energy between the two regimes is indicated by the dashed line.

The results reported in Fig. 6 indicate that lowering the landing energy, although helping with SNR in the specific case investigated of CAR on SOG, will also impact the charging characteristics of the surface, and this could have an impact by itself depending on the material under scrutiny.

2.4 Optimal LE for CAR

The positive impact of lowering the LE on CAR on SOG and UL1 is reported in Fig. 7. All the images in Fig. 7 were acquired by an Applied Materials PROVision 2E. In Fig. 7, a lower LE (300eV) as compared to the imec BKM used for Fig. 1 (500eV) is used. In Fig. 7(a) we observe that the LS pattern is clearly visible down to a target resist FT of 10nm, in contrast to what observed in Fig. 1(a). These results indicate clearly that lowering the LE does improve imaging in the case of CAR resist.

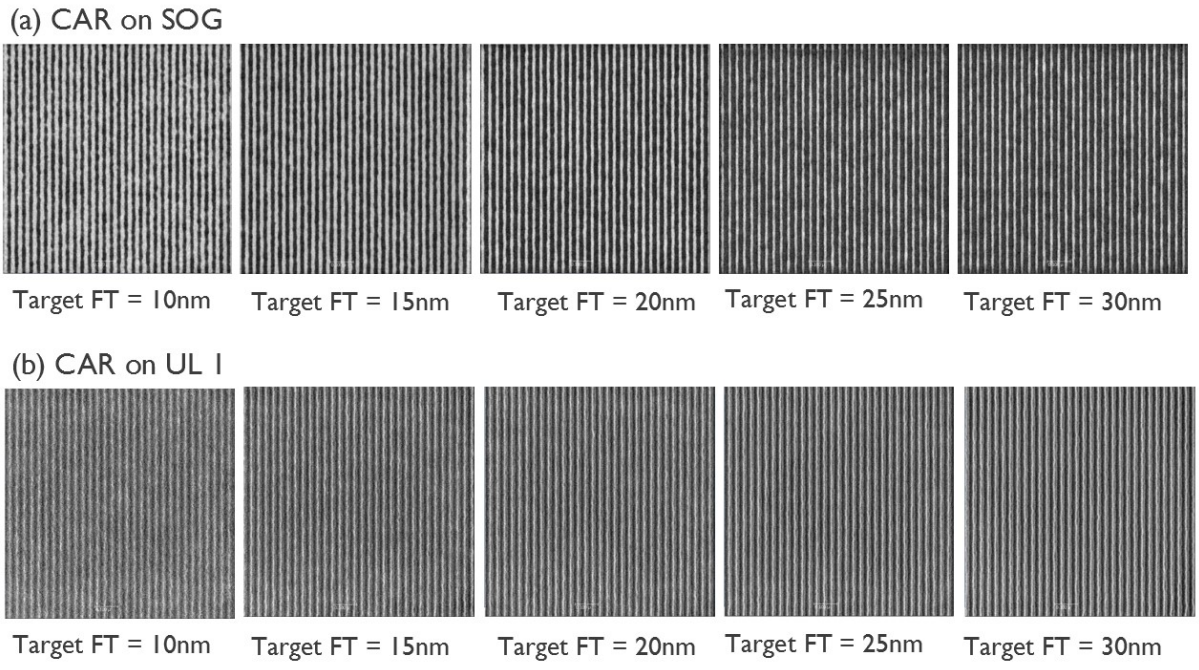

Figure 7. CAR resist wafers imaged in Fig.1, this time after optimizing the imaging condition for thin resist and using lower landing energy. The improvement in imaging is evident, particularly for the 10nm CAR on SOG case, where the pattern was not visible at 10nm Target FT. All images acquired by an Applied Materials PROVision 2E at 300eV LE.

2.5 Optimal LE for MOR

Although lowering the LE clearly improved image quality for CAR, this is not necessarily true for all types of resists. In Fig. 8, the results obtained at different LE (100eV and 300eV) for CAR (a) and MOR (b) on SOG by using an Hitachi CDSEM are reported. In this case, pitch 26nm and a CD of 12nm were targeted. Although imaging on CAR appears to perform better at low LE, the images on MOR appear to behave better at 300eV. Hence, the data in Fig. 8 indicate that there is not a unique solution for all cases. This is consistent with the difference observed between the two different organic UL in Fig. 2, where small differences in chemistry can bias the quality of the imaging results in different directions. In other words, our results indicate that LE is indeed an important knob required to define optimal BKM for thin resist, but also that there is no single setting that would be able to solve the problems for all resist and underlayer formulations.

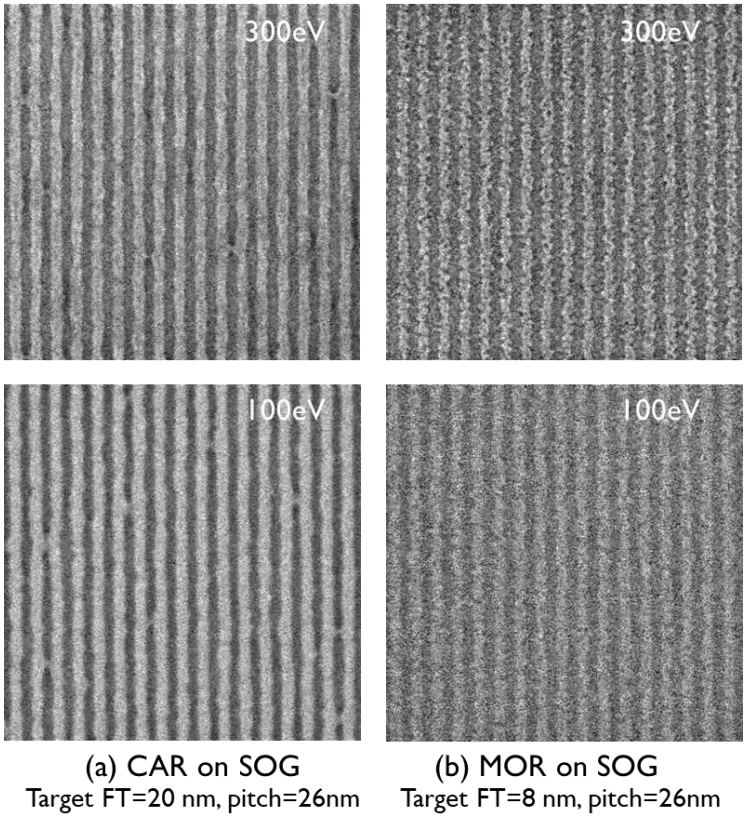

Figure 8. Images at different LE for CAR (a) and MOR (b) on SOG. Although imaging is improved for CAR at lower LE (100eV), this is not the case for MOR, where optimal results are obtained at higher LE (300eV). All images acquired by a Hitachi CDSEM.

2.6 Repeatability at different LE

Being able to image resist is important, but the most critical part of resist metrology is the ability to repeatably measure it. Hence, a critical point we need to clarify is related to what kind of performance it is possible to achieve with this LE setting in terms of repeatability. In Fig. 9, images obtained with optimal settings for CAR (a) and MOR (b) on UL1 for pitch 32nm features are reported. As discussed in section 2.5, in this case the optimal LE was found to 100eV for CAR and 300eV for MOR. In this case, we confirmed a dynamic repeatability of 0.12nm and 0.13nm for MOR and CAR using a Hitachi CDSEM, respectively, indicating that it is possible to achieve repeatability of about 0.1nm down to 100eV.

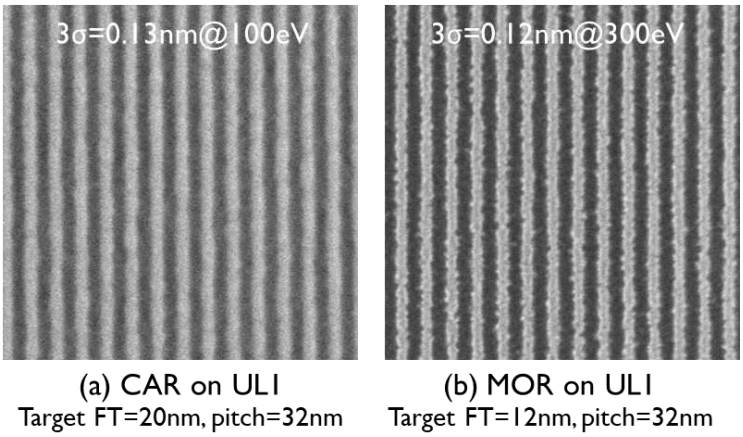

Figure 9. Optimized setting for CAR (a) and MOR (b) on UL1. In this case, we notice that while CAR tends to need low LE (down to 100eV), MOR works better with higher LE values (300eV) here. In both cases, the repeatability is on the order of about 0.1nm.

2.7 Impact of SNR on LWR metrology

To conclude this section on metrology of thin resist, it is important to discuss its impact on the quantification of another critical parameter, Line Width Roughness (LWR). As we reported, unbiasing of LWR estimate is critical to be able to distinguish in between measurement noise and actual patterning roughness [4-6]. However, as discussed in Chapter 2.1, one of the consequences of using thin resist consist in a possible decrease of the SNR in the images. The question we ask ourselves now is if this increased noise level is going to impact LWR metrology, and if so how.

To investigate the impact of reduced SNR on LWR metrology, we used simulated synthetic images (generated by MetroLER) having known LWR and adjustable SNR. Specifically, we used LWR of 2.5nm and SNR varying from 10 down to 1. We then measured the simulated images and estimated the unbiased LWR at different SNR levels. A measurement immune to the influence of the varying SNR would yield an accurate value (i.e., 2.5nm) independent of the noise level. In Fig.10(a) we plot the estimated unbiased LWR versus the SNR for simulated images. What we observe is a dramatic drop in the estimate when the SNR becomes smaller than 2. In this regime, an artificially low estimate is reported, making the result basically inaccurate.

In Fig. 10(b), we report the experimental verification of the simulated effect observed in Fig. 10(a). In this case we used CAR resist on different underlayers (SOG and UL1). The SNR was modulated even further by varying the number of averaging frames. Also in this case, we observe that the estimated values of unbiased LWR (measured by MetroLER) drops for SNR below 2, strongly suggesting a measurement artifact. From these results, we conclude that the estimates of unbiased LWR become less accurate as the SNR falls below 2, with an error as high as 30% when the SNR reaches 1.

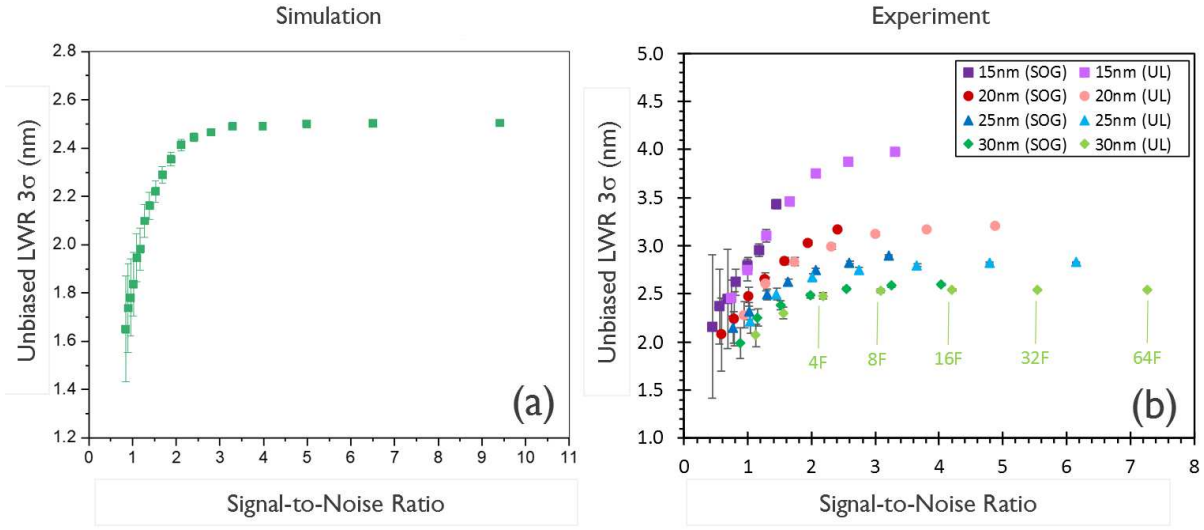

Figure 10. (a) Unbiased measurements of LWR on simulated images as a function of the SNR. The LWR input value used in the simulation is 2.5nm. For large SNR values, the measurement asymptotically converges to the accurate expected value of 2.5nm. However, when the SNR approaches 2 or below, an under-estimation of the LWR, up to 30%, is observed. (b) Experimental verification of the simulation results on CAR patterning, showing the drop in accuracy for SNR lower than 2.

3. RESULTS AND DISCUSSION - OPTICAL

3.1 Pattern Shift Response

After having investigated extensively the impact of using thin resist on e-beam metrology in Chap. 2, now we will investigate the consequences of such a choice on various optical metrology techniques, starting with pattern shift response (PSR) [7]. In Fig. 11(a) we report the optical images of the PSR targets at different target thickness for CAR and MOR on UL 1. Similar results were obtained on SOG. As in the case of e-beam (see Fig. 1), the optical images are observed to have less contrast for thinner resist, and the analysis is observed to fail in some extreme case (MOR on UL1 at a target FT of 12nm). However, by fine-tuning the wavelength, it is possible to measure the failing wafers too, as shown in Fig. 11(b).

The experimental results for PSR indicate that the underlaying trends for optical metrology are in some way similar to what we observed for e-beam: a reduction of contrast for thinner resist that can be recovered by changing some of the measurement settings.

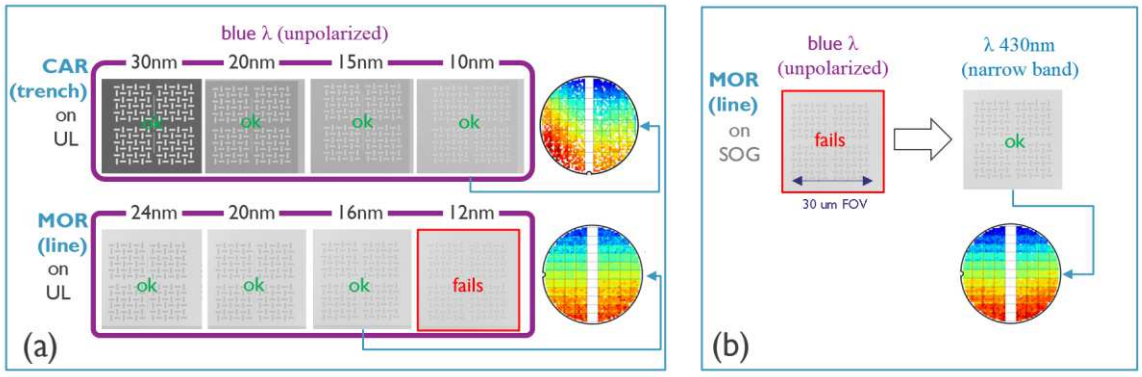

Figure 11. (a) Impact of film thickness on optical images of PSR targets for CAR and MOR, showing an issue for thin MOR. (b) The limitation of thin MOR resist can be solved using narrow band 430nm light.

3.2 Scatterometry

In this chapter we discuss the results obtained with NOVA scatterometry tool for CAR on SOG, at different target FT.

In Fig. 12(a) and 12(b) we discuss the FT scatterometry results. Fig. 12(a) shows the comparison between the results of scatterometry photoresist line thickness and AFM results, with good correlation between scatterometry results and reference metrology. In Fig. 12(b), the Optical CD (OCD) results at various target FT are shown, indicating a larger offset between actual and target FT for thicker film, also in this case in agreement with AFM results [8].

Fig. 12(c) shows a correlation plot between OCD and CDSEM results. Linearity and R^2 are nice, and we observe a small offset between CDSEM and OCD results, which is expected. No results are reported for 10nm target FT, as CDSEM measurement could not be done because of the poor BKM imaging. OCD measurements by contrast were successful, and the wafer fingerprint agreed with what was observed for the thicker films. In Fig. 12(d) we report the variability chart for OCD and CDSEM, also in this case in agreement with expectations.

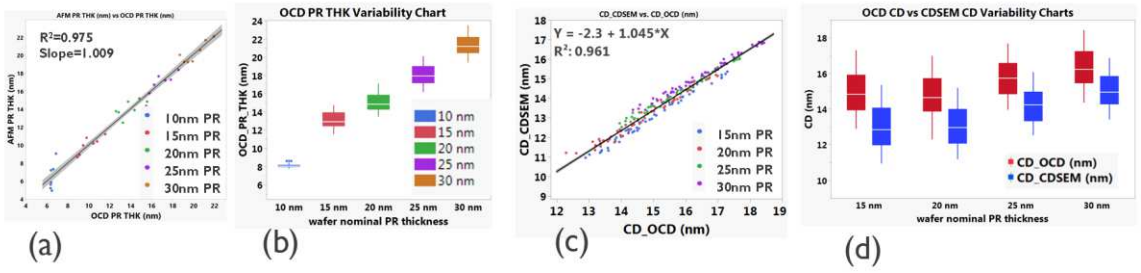

Figure 12. (a) Comparison between AFM and OCD thickness measurements of the patterned lines, showing good agreement between OCD and reference measurements. (b) Comparison between OCD measured thickness of patterned lines and targeted film thickness, showing a larger offset for thicker coating as compared to thinner coating. (c) Comparison between CDSEM and OCD CD measurement, showing very nice linearity. CD for 10nm Target FT could not be measured with CDSEM. (d) Comparison between CDSEM and OCD average CD, showing similar trend and an expected offset.

3.3 Optical Inspection.

To conclude, we discuss the impact of thin resist on optical inspection. In Fig. 13 we report the results for CAR at different target FT. The results were obtained using a KLA2935. The investigation was performed by evaluating the capture rate for bridges only, as the capture rate for breaks is usually extremely low. The results in Fig. 13 are for CAR on SOG, but very similar results were obtained for CAR on UL1.

We started with a row of programmed defects that are easily detectable for target FT of 30nm. The programmed defects were then investigated through target FT. The results in Fig. 13 indicates that, as the resist becomes tinner, the ability to detect defects is severely hampered, and although some defect can be detected at target FT of 20nm, no defect is visible anymore below 20nm.

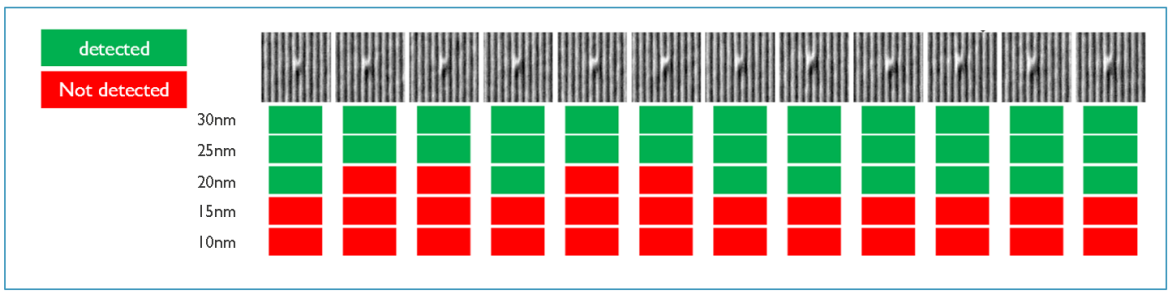

Figure 13. Impact of target FT on optical defect inspection for bridges. No defect is detected anymore below 20nm target FT.

4. CONCLUSIONS

We investigated the impact of reducing film thickness on various e-beam and optical metrology techniques.

In the case of e-beam metrology, our results indicate that the imaging noise level increases when decreasing film thickness. In addition, the noise level at similar SEM condition will depend on the material characteristics, and MOR was observed to have lower SEM image noise level than CAR resist, at least the specific formulations investigated. In addition, the noise level depends on the underlayer used, and it can vary also between underlayers of the same type but with different formulation. We also observed that SNR can be improved by tuning the landing energy in a proper way. We observed that CAR will perform better in terms of imaging at lower LE, while MOR will perform better at higher LE, at least the specific formulations investigated. Precisions for optimized LE settings for both CAR and MOR were found to be 0.1nm, in line with High NA EUVL requirements. Our results indicate that LE is a critical knob to be able to cope with low SNR arising from the use of thin resist. Finally, we noticed a relevant impact on LWR metrology accuracy when the SNR drops below 2, and it is suggested to perform unbiased LWR analysis only for SNR above 2, at least until a proper solution is identified for this regime.

With respect to optical metrology, in the case of scatterometry, our results demonstrated capability to measure both critical dimensions and photoresist line thickness in all studied cases. With respect to pattern shift response and optical defect inspection, we noticed that, as for e-beam, the contrast is observed to decrease with film thickness. However, for pattern shift response, it has been possible to find a suitable setting that would allow proper metrology. In terms of defect inspection, by contrast, we observe that it is not possible to detect defects below 20nm target FT with the tool we used.

In summary, our results indicate that the impact of thin film on both e-beam and optical metrology can be minimized by optimizing the working points of the technique in use.

5. ACKNOWLEDGEMENT

The wide variety of investigation reported in this work were only possible thanks to the dedication of many additional contributors from various companies.

- Yuta Kawamoto, Yuzuru Mizuhara, Makoto Suzuki, Wataru Mori, Toru Ishimoto, Takumichi Sutani, Shunsuke Koshihara (Hitachi)
- Peter de Schepper (inpria)
- Andrew Cockburn, Aviram Tam, Jens Van Hoof, Yaniv Abramovitz, (AMAT)

REFERENCES

[1] Gian Francesco Lorusso, Takumichi Sutani, Vito Rutigliani, Frieda Van Roey, Alain Moussa, Anne-Laure Charley, Chris Mack, Patrick Naulleau, Chami Perera, Vassilios Constantoudis, Masami Ikota, Toru Ishimoto, Shunsuke Koshihara, "Need for LWR metrology standardization: the imec roughness protocol," J. Micro/Nanolith. MEMS MOEMS 17(4), 041009 (2018),

[2] Michael Steigerwald, Christian Hendrich, Dirk Preikszas, Kai Schubert, "A mirror-Corrected scanning electron microscope", Proc. Frontiers of Characterization and Metrology for Nanoelectronics. 51-55 (2013)

[3] Mohamed Zidan, Daniel Fischer, Gian Francesco Lorusso, Joren Severi, Danilo De Simone, Alain Moussa, Angelika Müllender, Chris Mack, Anne-Laure Charley, Philippe Leray, and Stefa De Gendt, "Low-Voltage Aberration-Corrected SEM Metrology of Thin Resist for High-NA EUVL." SPIE Advanced Lithography, in press (2022)

[4] Chris A. Mack, and Gian F. Lorusso, "Determining the ultimate resolution of scanning electron microscope-based unbiasedroughness measurements. I. Simulating noise", Journal of Vacuum Science & Technology B, 37, 062903 (2019).

[5] Gian F. Lorusso, Vito Rutigliani, Frieda Van Roey, and Chris A. Mack, “Unbiased Roughness Measurements: Subtracting out SEM Effects, part 2”, Journal of Vacuum Science & Technology B, 36, 06J503 (2018).
[6] Chris A. Mack, Frieda Van Roey, and Gian F. Lorusso, “Unbiased Roughness Measurements: Subtracting out SEM Effects, part 3”, Proc. SPIE 10959, Metrology, Inspection, and Process Control for Microlithography XXXIII, 109590P (2019).
[7] Kit Ausschnitt, Vincent Truffert, Koen D'Have, Philippe Leray, “Pattern shift response metrology,” Proc. SPIE 10810, Photomask Technology 2018, 108100T (2018).
[8] Joren Severi, Gian F. Lorusso, Danilo De Simone, Alain Moussa, Mohamed Saib, Rutger Duflou, and Stefan De Gendt, “Chemically amplified resist CDSEM metrology exploration for high NA EUV lithography,” J. Micro/Nanopattern. Mater. Metrol. 021207-1, 21(2) (2022)